# Nonlinear reflectivity of strongly coupled exciton-photon systems under resonant and non-resonant pumping

A. L. Bradley[1,*], J. P. Doran[2], J. Hegarty[1], R. P. Stanley[3], U. Oesterle[3], R. Houdré[3] and M. Ilegems[3]
[1]*Physics Department, University of Dublin, Trinity College, Dublin 2, Ireland.*
[*]*Corresponding Author – Formerly of Trinity College. Current address: Institute of Technology Tallaght, Tallaght, Dublin 24, Ireland.*
*Telephone: 353-1-4042875 and E-mail: louise.bradley@it-tallaght.ie.*
[2]*Dublin Institute of Technology, School of Physics, Kevin Street, Dublin 8, Ireland.*
[3]*Institüt de Micro- et Optoélectronique, EPFL, CH-1015, Lausanne, Switzerland.*

## ABSTRACT

Coupled exciton-photon systems are investigated using the pump-probe technique in order to gain a better understanding of the important mechanisms governing cavity-polariton nonlinear behaviour and dynamics. A semi-classical model is used to describe the nonlinear behaviour and identify the dominant nonlinear mechanisms. Our phenomenological model produces very good agreement with experiment. The influence of free carriers on nonlinearities in the strong coupling regime was studied directly using non-resonant pump-probe.

**Keywords:** microcavity, cavity-polariton, non-linear, exciton.

## INTRODUCTION

The advent of semiconductor microcavities has presented the opportunity to investigate new and exciting phenomena in solid state structures. The basic concepts of microcavity operation were proposed as early as 1946 and were initially demonstrated in atomic systems [1, 2]. By controlling the number of allowed photon modes the light-matter interaction can be controlled. An atom inside a small sized cavity can exhibit modification of the spontaneous emission rate, spatial emission pattern and for a multi-wavelength source the cavity will act as a spatial filter. The cavity has a perturbative effect on the material system inside and the behaviour is within the range of validity of Fermi's Golden Rule. This is known as the weak coupling regime and the electronic states, atoms or exciton, are not altered by the presence of the cavity. The effects of weak coupling have been successfully exploited to enhance the performance of light emitting diodes [3, 4, 5]. There is another regime of operation in which the light-matter interaction is sufficiently strong to alter the fundamental energy levels of the optically active material. This is known as the strong coupling regime and has been an area of study in atomic systems for many years [6, 7, 8]. When an electronic state is sufficiently strongly coupled to a photon, energy is periodically transferred between the photon and material components of the state at a

rate determined by the Rabi frequency. The emission process is no longer described by Fermi's Golden Rule. The coherent transfer of energy from the electronic state to the photon state requires that the Rabi oscillations occur at a faster rate than the dephasing of the electronics state or the dephasing of the cavity-photon. Strong coupling, between the atomic-like exciton resonance and the cavity photon, was only first observed in monolithic semiconductor planar Fabry-Perot microcavity structures in 1992 [9]. The normal modes of the coupled system are a pair of mixed exciton-photon states, named cavity-polaritons [10]. The energy splitting between the two states is the Rabi splitting, $\Omega \propto \sqrt{f/L_{cav}}$, where $f$ is the oscillator strength of the exciton transition and $L_{cav}$ is the effective cavity length. The dynamics of the strongly coupled exciton-photon system are also fundamentally altered. In a simple coupled oscillator picture the decay rate of the cavity-polariton is given by

$$\frac{1}{\tau_{cp}} = \frac{1}{\tau_{exciton}} + \frac{1}{\tau_{photon}} \tag{1}$$

where $\tau_{cp}$ is the cavity-polariton decay time, $\tau_{exciton}$ is the exciton dephasing time and $\tau_{photon}$ is the dephasing time of the cavity-photon. When $\tau_{exciton} >> \tau_{photon}$ then $\tau_{cp}$ approximates to $\tau_{photon}$, which would result in ultra-fast behaviour.

Since the first demonstration of strong coupling in semiconductor systems there has been a flurry of experimental and theoretical work. Strong coupling between photons and atoms has been previously investigated and well understood. The systems have been successfully described using both a quantum mechanical mixed oscillator model [6, 11] and classical linear dispersion theory [8]. With semiconductor materials there are extra considerations such as the effects of the inhomogeneous broadening of the exciton resonance, exciton-exciton interactions and exciton-phonon interactions on the coupled system. Initial investigations focussed on obtaining an accurate physical description of the strongly coupled states. The classical linear dispersion theory by Zhu *et al* [8] has been successfully applied to predict the experimentally observed linear optical response of semiconductor microcavities [10, 12].

There has also been much interest in the nonlinear optical behaviour in the strong coupling regime. The excitation density dependence of the Rabi splitting has been examined by Jahnke *et al.* [13]. They reported strong broadening of the excitonic states with no significant loss of oscillator strength up to densities causing saturation of the exciton resonance, at which time a change from an

anti-crossing to crossing behaviour is observed in the linear transmission spectra. However, Houdré *et al.* [14] and Norris *et al.* [15] report a decrease in Rabi splitting with increasing density, ultimately resulting in a transition from strong to weak coupling operation. Using quantum field theory Hanamura has identified varying degrees of inhomogeneous broadening as the source of the diverse observations [16]. Houdré *et al* [14] successfully describe their experiment by implementing saturation of the oscillator strength in the classical model of Zhu *et al* [8]. It has also been previously demonstrated that a classical model based on linear dispersion theory can be used to successfully describe the spectral and dynamic nonlinearities in both the weak and strong coupling regimes [17].

In this paper the results of 2-laser non-degenerate pump-probe experiments are presented and a significant modification of the nonlinear spectral properties is observed. The central question we address is whether the semi-classical model which was applied to the resonant pumping case can be further adapted to describe the non-resonant pump-probe experimental results. The paper is divided into two main sections. For the purposes of clarity and comparison, a review of strong coupling nonlinear behaviour under conditions of resonant pumping is presented. The non-resonant pump-probe experiment and results are introduced in the next section. This is followed by a discussion on the modification of the model required to render it suitable for description of free-carrier excitation.

## SAMPLE

The sample is a planar Fabry-Perot type structure, grown using molecular beam epitaxy technology. The mirrors are multiple quarter-wave stack distributed Bragg reflectors (DBRs) in which the low (high) index material is AlAs($Al_{0.1}Ga_{0.9}As$). The $3\lambda/2$ cavity contains 6 $In_{0.87}Ga_{0.13}As$ quantum wells, placed in two groups of three at the two available electric field anti-nodes. There are 6 and 9.5 pairs in its front and back mirrors respectively. A schematic of the sample is presented in figure 1(a). The wafer was not rotated during the growth of the cavity layer which results in a wedge shaped cavity, allowing for detuning of the exciton and cavity resonances by moving across the sample. The presence of an anti-crossing, rather than a crossing, of the exciton and cavity resonances at zero detuning indicates the strong coupling nature of the interaction, as presented in figure 2(a).

## RESONANT PUMP-PROBE

### Experiment

Degenerate pump-probe was performed in the reflection geometry as illustrated in figure 1(b). The laser source is a synchronously modelocked Nd:YAG pumped Styryl-13 dye laser producing 70 ps pulses in the 900 nm to 960 nm wavelength range. The dye laser output is split into the pump and probe beams. The probe is delayed with respect to the pump using a retro-reflecting delay line for the dynamical measurements. The reflected probe is detected using a cooled photo-multiplier tube and a cascaded lock-in amplifiers arrangement. The output is a measure of the differential reflectivity, $\Delta R$, which is positive in the case of an increase in the reflectivity over the linear reflectivity and negative in the case of a decrease. For all pump-probe measurements the samples were held at 7 K in a closed cycle helium cryostat and at the position of zero detuning between the exciton and cavity resonances.

### Results and analysis

The linear reflectivity, recorded at the resonance position, using the probe beam is presented in figure 2(a). The anti-crossing behaviour at zero detuning resulting in a Rabi splitting of 7.2 meV confirms strong coupling operation. It is also worth noting the asymmetry in the linewidths of the two peaks, the higher energy line broader than the low energy one. This originates from coupling to the continuum and to excited exciton states. Simulations including coupling to the 2s exciton states result in broadening of the high energy line [10]. Nonlinear (differential) reflectivity spectra recorded at zero time delay between the pump and probe pulses, for a range of pump intensities are presented in figure 2(b). There is a change in the magnitude of the signal with increasing pump intensity but not much variation in shape.

Due to the successful application of linear dispersion theory to simulation of the linear optical spectra [10], our first approach to modelling the nonlinear behaviour was to extend the linear dispersion theory to this regime. We have shown previously that the simple dispersion theory applied to modelling nonlinear behaviour in the weak coupling regime brought about a striking agreement with the experimental data [17]. The question of whether such an approach could also be successfully applied to a structure operating in the strong coupling regime was also addressed. A review of the model developed and its application to the strong coupling regime is presented below.

### Model

This approach is implemented in the form of a transfer matrix model, which is used to calculate the electric-field intensity at all positions within the microcavity structure, as well as the absorption, reflectivity and transmission spectra. The quantum well exciton is included in the form of a Lorentz oscillator with a dispersive dielectric constant, $\varepsilon$:

$$\varepsilon(\mathrm{E}) = \varepsilon_{\infty} + \frac{fq^2\hbar^2}{m\varepsilon_0 L_z}\frac{1}{E_X^2 - E^2 - i\Gamma_h E} \tag{2}$$

where $E$ is the energy, $f$ is the oscillator strength per cm$^2$, $q$ is the charge, $m$ the mass, $E_X$ the energy of the exciton resonance, $\Gamma_h$ the homogeneous exciton linewidth and $L_z$ the quantum-well thickness. The dielectric constant yields the refractive index, the complex part of which is the absorption due to the exciton resonance. Inhomogeneous broadening, arising from alloy broadening and quantum well thickness fluctuations, is included as a Gaussian distribution of the oscillator energies. The linear exciton parameters for the sample, obtained by fitting the experimental reflectivity spectrum, are $E_{x0}$=1.334 eV, $f_0$=5.4×10$^{12}$ cm$^{-2}$, a homogeneous exciton linewidth $\Gamma_{h0}$=0.05 meV, and an inhomogeneous linewidth, $\Gamma_{inh}$ = 3 meV. The resulting theoretical spectrum is presented on the right-hand side of figure 2(a). The above classical description of the exciton in a quantum well is not valid for all well thicknesses but in the samples we are dealing with it provides good agreement with the measured linear spectra.

Within our model we assumed that some or all of the exciton parameters are altered by the presence of the high intensity pump and this results in a modified reflectivity spectrum for the whole microcavity structure. The nonlinear differential reflectivity spectrum corresponds to the difference between this new spectrum and the original linear spectrum. The nonlinear behaviour of excitons in quantum wells has been comprehensively examined [18, 19]. For resonantly excited excitons the mechanisms causing nonlinear behaviour are phase space filling and the exchange interaction. The impact of these two effects on the oscillator strength can be described by:

$$f = \frac{f_0}{1 + I_{qw}/I_{sat}} \tag{3}$$

where $f_0$ is the linear exciton oscillator strength, $f$ is the nonlinear oscillator strength, $I_{qw}$ is the intensity at the quantum well and $I_{sat}$ is a saturation intensity [20]. This equation can also be expressed in terms of the density, $N$ and a saturation density $N_s$ [19]. In quantum wells the nonlinear interactions also

result in a blue shift of the exciton resonance. The exact form of the dependence of this excitonic blue shift is not known – in the course of this work the best agreement with experiment was found by using a quadratic dependence:

$$\delta E_X = bI_{qw}^2 \tag{4}$$

where $b$ is a constant. At very high excitation densities the exciton blue shift will become comparable to the exciton binding energy in which case the exciton dissociates. The above equation is therefore only meaningful for exciton blue shifts which are smaller than the binding energy. Finally, broadening of the exciton homogeneous linewidth can occur as a result of scattering with other excitons, phonons, free carriers, lattice impurities or disorder. The density dependence of the exciton homogeneous linewidth can be expressed as:

$$\Gamma_h(N) = \Gamma_h(0) + \gamma N_{qw} \tag{5}$$

where $\gamma$ is the exciton-free carrier or exciton-exciton scattering efficiency, $N$ is the excitation density, $\Gamma_h(0)$ is the density independent homogeneous linewidth due to scattering by phonons, lattice impurities or disorder [21].

An adequate description of our experimental data also requires incorporation of the dynamical evolution of the reflectivity over the timescale of the 70 ps excitation pulse, incident on a cavity, which has a response time of the order of 1 ps (the photon lifetime). Consider at one instant along the pulse an intensity incident on the microcavity of $I_{inc}$. There will be a distribution of the electric field inside the cavity and a corresponding intensity, $I_{qw}$, at the quantum well position. The nonlinear nature of the exciton means that a change in intensity results in a change of the exciton parameters and the complex refractive index of the quantum well material is thus altered. Consequently the reflectivity of the structure is modified. The light arriving at the next instant along the pulse will experience a cavity with altered properties. Hence there is a dynamical evolution of the reflectivity over the duration of the pulse. The electric field distribution inside the cavity is also sensitive to wavelength, resulting in a spectral dependence of the nonlinear behaviour.

In summary the flow of our model is as follows: the initial parameters of the model are those which reproduce the linear reflectivity. Progressing across the pulse to the peak in 1 ps steps, at each step the quantum well intensity is calculated for each wavelength over the spectrum. Using equations (3), (4) and (5) the new spectrally dependent exciton parameters are calculated and subsequently fed

back into the model for the next instant along the pulse. Via this iterative process, a final reflectivity spectrum is obtained. Subtraction of the linear reflectivity spectrum yields the calculated nonlinear reflectivity spectrum.

The model can now be applied to simulating the resonant pump-probe experimental results. There are two fitting parameters, the saturation intensity, $I_s$, or saturation density, $N_s$, for determining the nonlinear oscillator strength and the parameter $b$ in equation 4 for determining the exciton blue shift. For resonant pumping we find that broadening of the exciton resonance is a relatively unimportant nonlinearity in these samples. We find a saturation density of $N_s = 2.9 \times 10^{10}$ cm$^{-2}$, which corresponds closely to that reported by Houdré et al [22], and a constant $b = 4.9 \times 10^{-20}$ nm/(cm$^{-2}$)$^2$. These parameters are also in exact agreement with those obtained in the simulation of the weak coupling pump-probe data [17]. A comparison of the experimental and theoretical spectra is presented in figure 2(b). The values of $I_{sat}$ and $b$ are held constant throughout and the incident intensity is varied in accordance with the experimental conditions. There are no other variables in the model. It is clear from a comparison of the simulated spectra with the experimental ones that the qualitative agreement at each pump intensity is significant. All the features evident on the experimental spectra, labelled A - L, are reproduced. It is perhaps surprising in our simple model that even a series of small features ($E_1$ - $E_3$) come directly from the calculations. It is not straightforward to correlate each of these features directly with a physical parameter. Although our model is simple in principle, the implementation of the bleaching and blue-shifting in the dynamical picture outlined above is complex and the origin of each feature in the spectrum not easily described. There are slight discrepancies between theory and experiment which is perhaps due to the fact that the linear reflectivity spectrum is not reproduced exactly in the calculations.

Time-resolved pump-probe experiments have also been performed. The evolution of the nonlinear reflectivity at two wavelengths is presented, with an incident intensity of $I_{inc}$=3.66 × 10$^2$ Wcm$^{-2}$ in both cases, in figure 3. The wavelength positions are indicated on figure 2(a). The evolution of the nonlinear signal depends critically on wavelength. The simplest approach to adapting the model to simulation of the time-resolved behaviour is to assume that the dynamics of the nonlinear behaviour are governed by the decay of the carrier population. Using time-resolved photoluminescence (see inset on figure 3), performed on this sample at the same temperature and density of excitation as the pump-

probe measurements, the decay of the density was found to be exponential with a decay constant of 900 ps [23]. The temporal evolution of the exciton oscillator strength and energy blue shift can now be determined and hence that of the nonlinear reflectivity. The calculated decays are compared with the experimental data in figure 3. The complex behaviour comes directly from the model and there is again good correspondence between the theoretical and experimental results.

**Discussion**

It is clear that there is good agreement between the experimental spectra and those resulting from the classical modelling approach. Although there are many features in the nonlinear spectra, which result from the interplay of the exciton and the cavity, the underlying physics is unchanged from that of bare quantum well excitons. The validity of applying this classical theory to strong coupling microcavities has previously been illustrated by its successful description of the linear behaviour. Our results have shown that, perhaps surprisingly, such a classical model can also be directly extended to nonlinear behaviour in strong coupling microcavitites.

The dynamics observed in the time-resolved pump-probe measurements presented above result from the decay of the excited population which occurs on the timescale of hundreds of picoseconds, as measured using the time-resolved photoluminescence technique.

## NON-RESONANT PUMP-PROBE

Two laser pump-probe measurements were performed with a view to investigating the impact of non-resonant pumping on nonlinear behaviour in the strong coupling regime. The experimental set-up is similar to that for the resonant experiments except that now the pump pulse comes from a second independent dye laser. The probe beam investigates the changes induced by the pump excitation, which occurs at a single wavelength. The nonlinear detection system is the same as for the single laser case and again all measurements were performed at 7 K.

A series of experimental nonlinear reflectivity spectra are presented on the left hand-side of figure 4(b), with the pump wavelength decreasing from 931 nm, which is resonant with the low energy Rabi spilt resonance, to 912 nm which corresponds to pumping in the continuum. The same incident intensity, $I_p$ = 732 Wcm$^{-2}$, is used in all cases and the spectra are recorded under the condition of zero time delay between the pump and probe pulses. The magnitude of the nonlinear signal, decreasing with decreasing pump wavelength, is attributed broadly to the increasing reflectivity resulting in a

lower excitation intensity at the quantum well. Pumping at 931 nm, the shape of the spectrum is similar to what was observed for the single laser case (shown for comparison in figure 4 (a)). However as the pump wavelength is decreased we see the emergence of a new negative feature on the high wavelength side of the spectra.

**Model and discussion**

As a first step to investigating the nonlinear behaviour in the non-degenerate pump-probe experiment, the dynamical model outlined above for the single laser measurements has been adapted for the two-laser case. The probe beam measures the changes induced by the pump excitation, which occurs at a different wavelength. Therefore the electric field distribution and corresponding intensity, $I_{qw}$, at the quantum well, which modifies the refractive index of the layer, has only to be calculated for the pump wavelength. As before the change in $I_{qw}$ results in an alteration of the reflectivity of the structure which is experienced by the probe.

Pumping non-resonantly, at energies above the band-gap, electron-hole pairs are created. Such excitation will effect the exciton resonance in a different manner to resonantly excited excitons and the resulting changes in the dominant mechanisms have to be taken into account in the model. At low temperatures both the phase space filling and exchange effects due to free carriers are larger than those associated with excitons because plane wave states have a larger overlap with a given bound state than other bound states. Free electron-hole pairs are approximately twice as efficient as bound pairs in bleaching the exciton resonance. Therefore, the saturation intensity used for calculating the oscillator strength in the model is approximately halved. The blue shift of the exciton resonance, which comes about due to exciton-exciton interactions has been shown to be absent under non-resonant pumping conditions when the excitons are interacting with electron-hole pairs. Finally, the effect of electron-hole pairs on the linewidth of the exciton resonance must be considered. Collisional broadening due to electron-hole pairs is expected to be much greater than that of resonantly created excitons due to their greater kinetic energy. It has been suggested that free carrier-delocalized exciton scattering is approximately ten times more efficient than delocalized exciton-delocalized exciton scattering [24].

The model was initially applied to the simulation of the pump-probe spectrum recorded for pumping at 931 nm. This corresponds to resonant excitation of excitons by the pump and hence, as a first approximation the parameters used to describe the exciton nonlinearities should be unchanged

from the resonant pump-probe case. Therefore, a saturation density of $N_s = 2.9 \times 10^{10}$ cm$^{-2}$, used to describe the saturation of the oscillator strength, and a constant $b = 4.9 \times 10^{-20}$ nm/(cm$^{-2}$)$^2$, used to describe the blue shift of the exciton, were employed. Broadening of the exciton resonance had been found to be negligible. There is good agreement between the resulting theoretical spectrum and the experimental data with all the main features being produced, as presented in figure 4(b). As was observed under resonant pumping there are some discrepancies in the relative sizes of some of the spectral features, which may be due to the fact that an exact fit of the linear reflectivity spectrum was not achieved.

Pumping at 912 nm more if the incident light is reflected off the sample than at 931 nm. This causes a significant reduction of the intensity at the quantum well and as a result there is negligible saturation of oscillator strength, even taking into account the fact that electron-hole pairs are twice as effective bleaching the exciton resonance. It became immediately apparent in our calculations that broadening of the exciton resonance is the only mechanism which can produce a negative feature at high wavelengths. It also became clear in the course of this work that it is necessary to consider an energy dependent distribution of the homogeneous linewidth. Such a distribution is phenomenologically included in our model in order to reproduce the experimental spectrum for a pump wavelength of 912 nm. The lower scattering efficiency limit is that used in the resonant pump-probe simulations and corresponds to $\gamma = 1.59 \times 10^{-7}$ μeVcm$^2$. This value agrees well with previously reported exciton-exciton scattering efficiencies [24]. In order to produce a nonlinear spectrum similar in magnitude and shape to the experimental spectrum the scattering efficiency is changed by a factor of 100 over the exciton resonance, corresponding to an upper scattering efficiency limit of $\gamma = 1.59 \times 10^{-5}$ μeVcm$^2$. This indicates that free carrier-localized exciton scattering is approximately 100 times more efficient than localized exciton-localized exciton scattering.

We emphasize that the inclusion of such a distribution of the homogeneous linewidth is phenomenological. Other researchers have performed FWM measurements on a very similar strong coupling sample to ours – one which has a higher finesse cavity but is identical in all other respects [25]. Their measurements were spectrally resolved and they found that in order to explain their experimental data a variation of the homogeneous linewidth across the inhomogeneous exciton resonance had to be included, just as with our results. Such a variation of the homogeneous linewidth across the resonance is, of course, well known in quantum well structures, and corresponds sometimes

to a change from localized excitons in the low energy tail to delocalized excitons above a so-called mobility edge.

## CONCLUSION

In this paper an overview of pump-probe experiments performed to investigate cavity-polariton nonlinear behaviour and dynamics is presented. Spectral and dynamic differential reflectivity measurements in the strong coupling regime have been described using a semi-classical model which is an extension of the linear dispersion theory approach previously used to predict linear optical properties. There is notable agreement between experiment and theory over a range of pump intensities. The interpretation of our results is that the nonlinear behaviour in the strong coupling regime can be described quite simply in terms of the nonlinearities associated with the bare quantum well exciton. The dominant mechanisms producing the nonlinearity under conditions of resonant pump and probe beams are found to be saturation of the exciton strength and blue shifting of the exciton energy. There is, however, no significant broadening of the homogeneous linewidth required to generate the spectra. The nonlinear dynamics were determined by the decay of the population as measured directly using photoluminescence. The influence of free carrier excitation on the nonlinear behaviour was examined via non-resonant pump-probe experiments. We have also extended the semi-classical modelling approach to describe the modification of the nonlinear properties in the presence of free carriers. It was clearly seen that collisional broadening of the exciton homogeneous linewidth becomes a dominant nonlinear mechanism in this case of non-resonant pumping. We also find a necessity of including a distribution of exciton scattering efficiencies in the non-resonant pump-probe modelling. This is consistent with the measurements of Bongiovanni *et al* [25]. Furthermore, an upper limit on the scattering efficiency of $\gamma = 1.59 \times 10^{-5}$ $\mu eVcm^2$ was extracted, indicating that free carrier-localized exciton scattering is 100 times more efficient than exciton-exciton scattering. This number is, of course, only approximate due to the uncertainties in the experiments and the phenomenological nature of the model. Our studies have demonstrated the perhaps surprising effectiveness of a classical modelling approach to describing many aspects of the nonlinear behaviour of a strongly coupled exciton-photon system.

**List of figures**

Fig. 1. a) Schematic showing structure of strong coupling microcavity; b) the pump-probe experimental set-up.

Fig. 2. a) Experimental (left hand side) and theoretical (right hand side) linear reflectivity spectra; b) experimental and theoretical nonlinear reflectivity spectra at varying pump intensities ($\tau$=0).

Fig 3. Experimental (left hand side) and theoretical (right hand side) evolution of the nonlinear reflectivity at two different pump wavelengths (as indicated on figure 2(a)). The inset in the centre of the figure shows the decay of the photoluminescence as a function of time, with a decay constant of 900 ps.

Fig. 4. a) Experimental (left hand side) and theoretical (right hand side) resonant pump-probe nonlinear reflectivity spectrum; b) experimental (left hand side) and theoretical (right hand side) non-resonant nonlinear reflectivity spectra at two pump wavelengths, 931 nm and 912 nm.

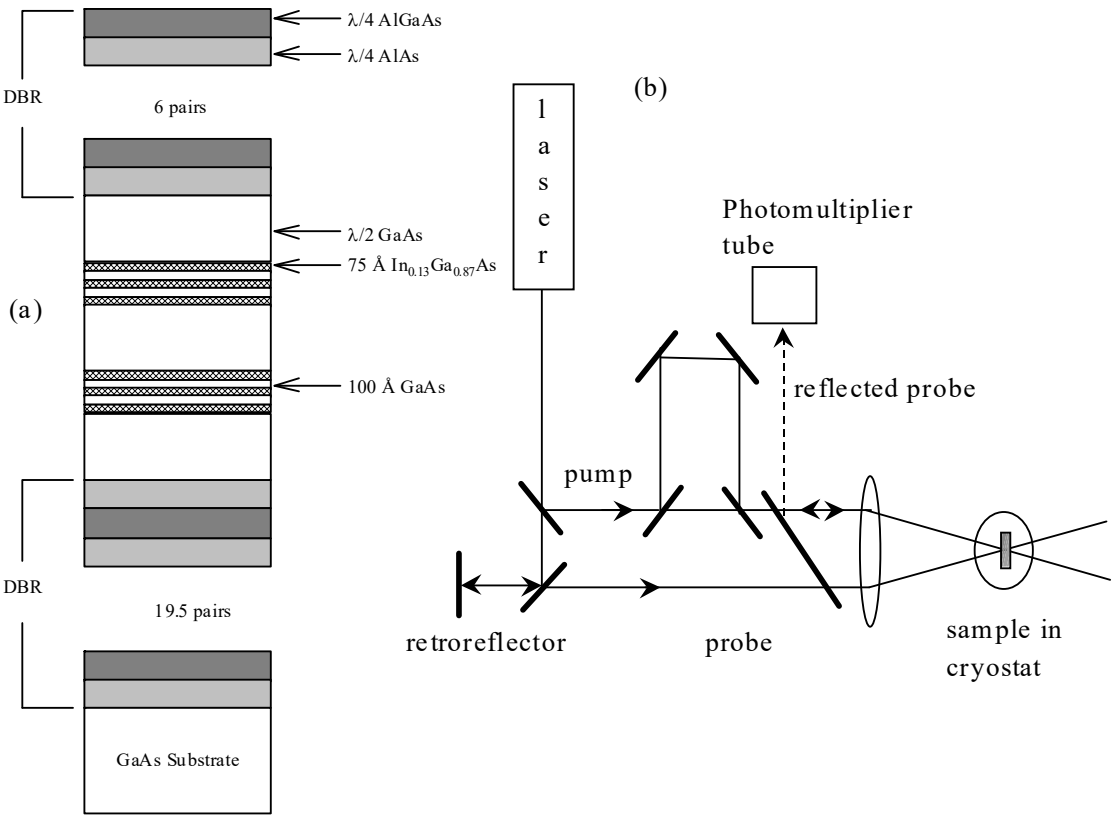
λ/4 AlGaAs
λ/4 AlAs
DBR
6 pairs
λ/2 GaAs
75 Å $In_{0.13}Ga_{0.87}As$
100 Å GaAs
(a)
DBR
19.5 pairs
GaAs Substrate
(b)
laser
Photomultiplier tube
reflected probe
pump
retroreflector
probe
sample in cryostat

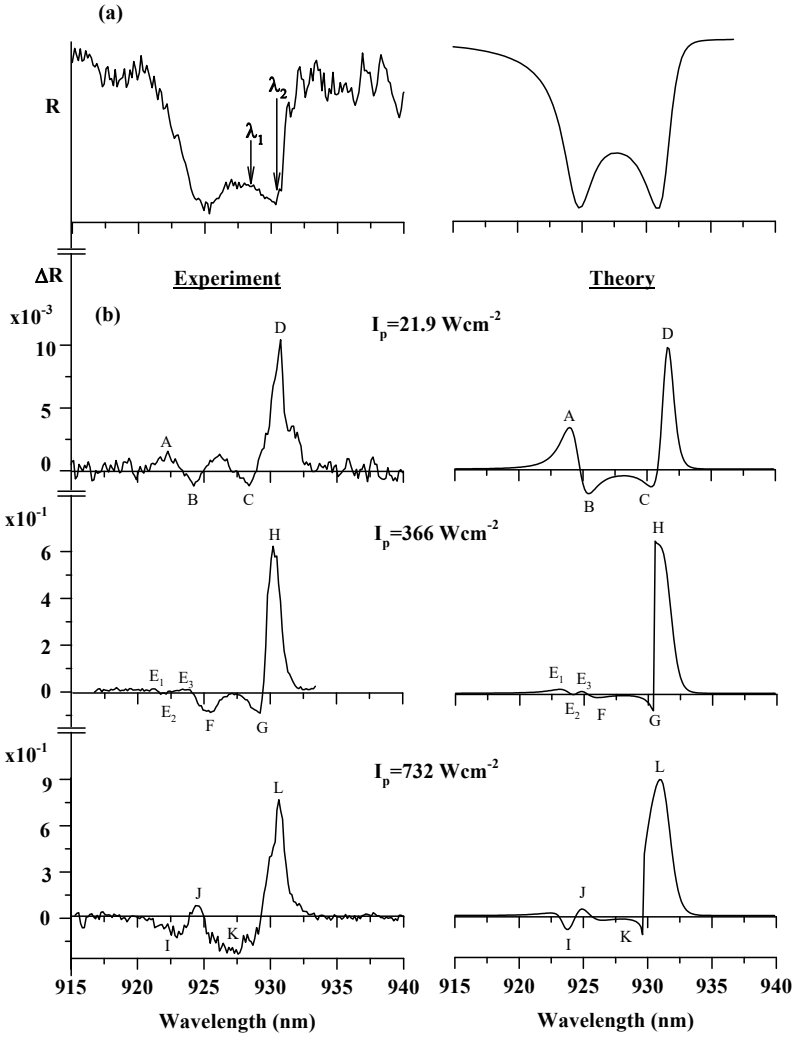
(a)
R
λ2
λ1
ΔR
Experiment
Theory
(b)
x10-3
10
5
0
Ip=21.9 Wcm-2
D
A
B
C
x10-1
6
4
2
0
Ip=366 Wcm-2
H
E1
E3
E2
F
G
x10-1
9
6
3
0
Ip=732 Wcm-2
L
J
I
K
915
920
925
930
935
940
Wavelength (nm)

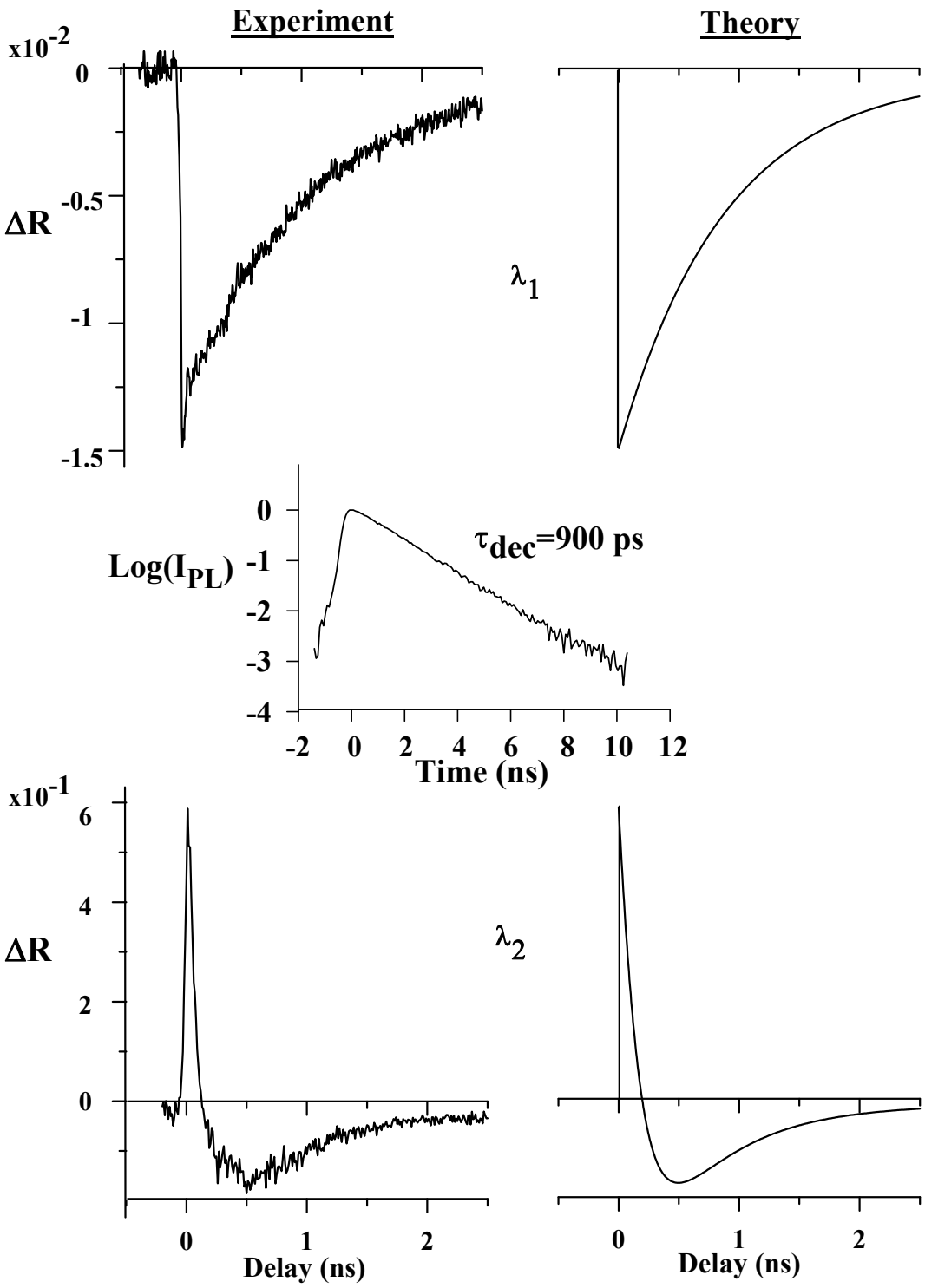
Experiment
Theory
x10-2
0
-0.5
-1
-1.5
ΔR
λ1
Log(IPL)
0
-1
-2
-3
-4
τdec=900 ps
-2
0
2
4
6
8
10
12
Time (ns)
x10-1
6
4
2
0
ΔR
λ2
0
1
2
Delay (ns)
0
1
2
Delay (ns)

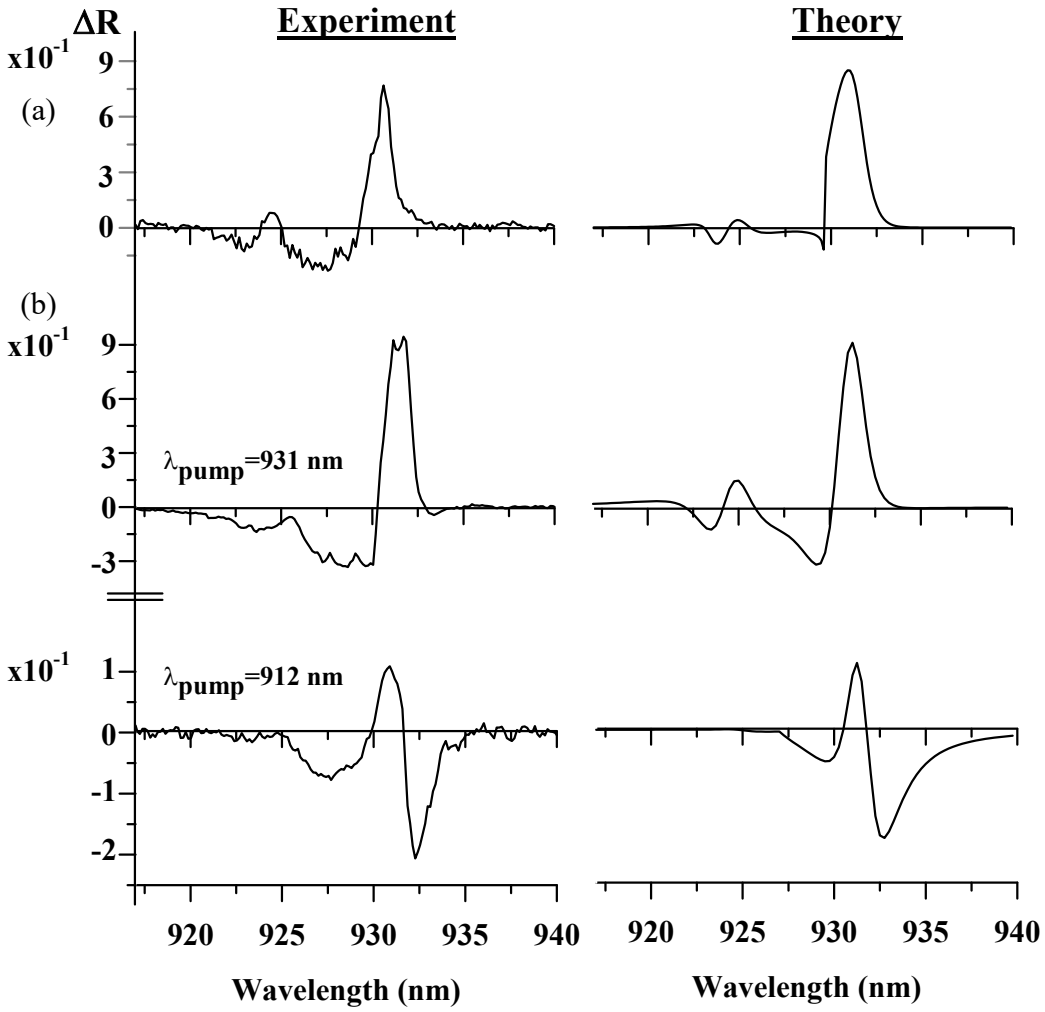
ΔR
Experiment
Theory
x10-1
9
6
3
0
(a)
(b)
x10-1
9
6
3
0
-3
λpump=931 nm
x10-1
1
0
-1
-2
λpump=912 nm
920
925
930
935
940
Wavelength (nm)
920
925
930
935
940
Wavelength (nm)

## REFERENCES


1. E. M. Purcell, Phys. Rev. **69**, 681 (1946).
2. D. J. Heinzen, J. J. Childs, J. E. Thomas and M. S. Feld, Phys. Rev. Lett. **58**, 1320 (1987).
3. J. Blondelle, H. De Neve, P. Deemester, P. Van Daele, G. Borghs and R. Baets, Electron. Lett. **31**, 1286 (1995).
4. H. de Neve, J. Blondelle, P. Van Deale, P. Demeester, R. Baets and G. Borghs, Appl. Phys. Lett. **70**, 799 (1997).
5. K. Streubel, U. Helin, V. Oskarsson, E. Bäcklin and Å. Johansson, IEEE Photonics Technol. Lett. **10**, 1685 (1998).
6. R. P. Berman, Cavity quantum Electrodynamics, (Academic Press, Boston, 1994).
7. G. S. Agarwal, J. Opt. Soc. Am., B **2**, 4800 (1985).
8. Y. Zhu, D. J. Gauthier, S. E. Morin, Q. Wu, H. J. Carmichael and T. Mossberg, Phys. Rev. Lett. **64**, 2499 (1990).
9. C. Weisbuch, M. Nishisoka, A. Ishikawa and Y. Arakawa, Phys. Rev. Lett. **69**, 3314 (1992).
10. R. Houdré, R. P. Stanley, U. Oesterle, M. Ilegems and C. Weisbuch, Phys. Rev. B **49**, 16761 (1994).
11. S. Haroche and D. Kleppner, Physics Today **43**, 24 (1989).
12. R. Houdré, C. Weisbuch, R. P. Stanley, U. Oesterle, P. Pellandini and M. Ilegems, Phys. Rev. Lett. **73**, 2043 (1994).
13. F. Jahnke, M. Kira, S. W. Koch, G. Khitrova, E. K. Lindmark, T. R. Nelson, Jr., D. V. Wick, J. D. Berger, O. Lyngnes, H. M. Gibbs and K. Lai, Phys. Rev. Letts. **77**, 5257 (1996).
14. R. Houdré, J. L. Gibernon, P. Pellandini, R. P. Stanley, U. Oesterle, C. Weisbuch. J. O'Gorman, B. Roycroft and M. Ilegems, Phys. Rev. B. **52**, 7810 (1995).
15. T. B. Norris, J.-K. Rhee, C.-Y. Sung, Y. Arakawa, M. Nishioka and C. Weisbuch, Phys. Rev. B **50**, 14663 (1994).
16. E. Hanamura, Microcavities and Photonic Bandgaps: Physics and Applications p.533 (Kluwer, 1996).
17. A. L. Bradley, J. P. Doran, T. Aherne, J. Hegarty, R. P. Stanley, R. Houdré, U. Oesterle and M. Ilegems, Phys. Rev. B **57**, 9957 (1998).
18. S. Schmitt-Rink, D. S. Chemla and D.A.B. Miller, Advances in Physics **38**, 89 (1989).
19. S. Schmitt-Rink, D.S. Chemla and D.A.B. Miller, Phys. Rev. B **32**, 6601 (1985).
20. A. Miller, D.A.B. Miller and S.D. Smith, Advances in Physics **30**, 697 (1981).
21. T. Takagahara, J. Lumin. **44**, 347 (1989).
22. R. Houdré, J. L. Gibernon, P. Pellandini, R. P. Stanley, U. Oesterle, C. Weisbuch. J. O'Gorman, B. Roycroft and M. Ilegems, Phys. Rev. B. **52**, 7810 (1995)
23. B. Roycroft, Ph. D. Thesis.
24. L. Schultheis, J. Kuhl, A. Honold and C. W. Tu, Phys. Rev. Lett. **57**, 1635 (1986).
25. G. Bongiovanni, A. Mura, F. Quochi, S. Gürtler, J. L. Staehli, F. Tassone, R. P. Stanley, U. Oesterle and R. Houdré, Phys. Rev. B **55**, 7084 (1997).